CONSTRAINING NUCLEAR SYMMETRY ENERGY WITH RELATIVISTIC ISOBAR COLLISIONS

HAOJIE XU (徐浩洁)

HUZHOU UNIVERSITY(湖州师范学院)

THE 16TH WORKSHOP ON QCD PHASE TRANSITION AND RELATIVISTIC HEAVY-ION PHYSICS

24-28TH OCTOBER, 2025, GUILIN

Nuclear symmetry energy

In nuclear EOS, the energy per nucleon $E(\rho,\delta)\equiv E(\rho,0)+E_{\rm sym}\delta^2+..$

Where ρ is density, and $\delta\equiv(\rho_n-\rho_p)/\rho$. Expanded around ρ_0 (or sub-saturation density $\rho_c\approx 2\rho_0/3$)

$$L(\rho_0)\equiv 3\rho_0\left(\frac{dE_{\rm sym}}{d\rho}\right)_{\rho_0} \qquad L(\rho_c)\equiv 3\rho_c\left(\frac{dE_{\rm sym}}{d\rho}\right)_{\rho_c}$$

- Stiff symmetry energy: $E_{\rm sym}$ increase rapidity with density, large L
- Soft symmetry energy: $E_{\rm sym}$ increase slowly/saturate at high density, small L

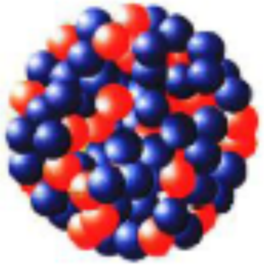
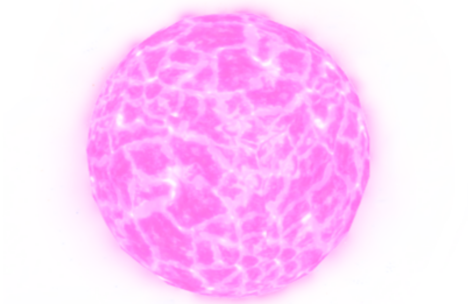

Key to a unified description of nuclear physics, from the smallest to the largest scales.

Nuclear symmetry energy in nucleus

The binding energy

$$B(A,Z) = a_V A + a_S A^{2/3} + a_C \frac{Z(Z-1)}{A^{1/3}} + a_A \frac{(N-Z)^2}{A}$$

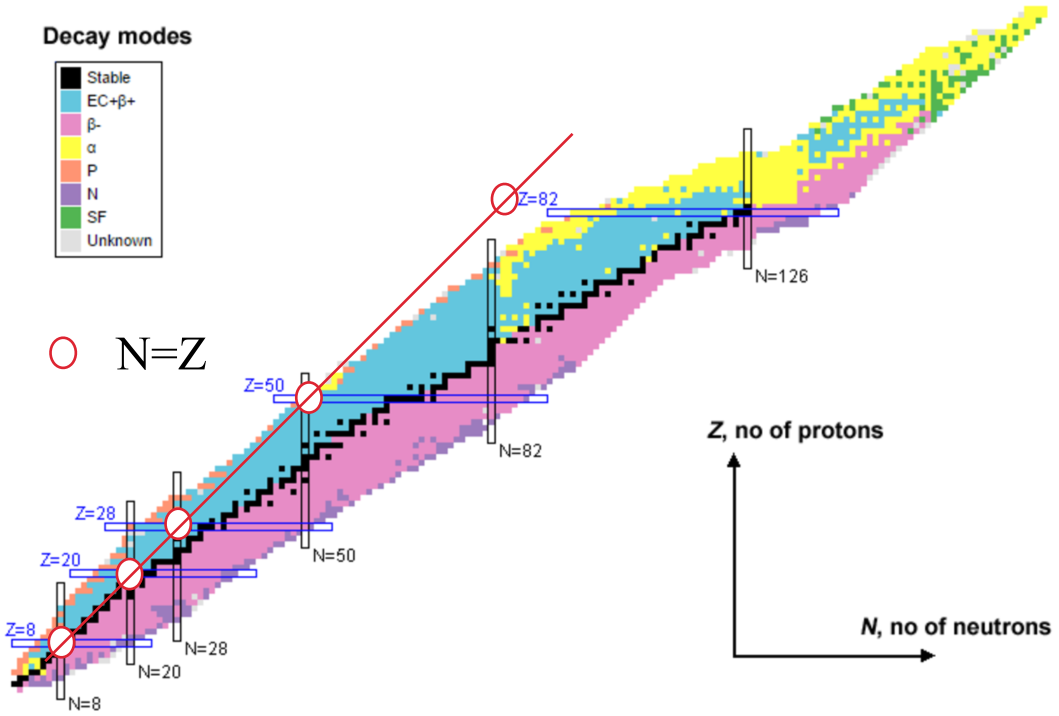

- For light nuclei, the Coulomb repulsion is weak, N ≈ Z
- For heavy nuclei, Coulomb repulsion is very strong, N > Z
    - More strong force against Coulomb force
    - Penalty from symmetry energy
    - The competition between the instability from Coulomb and symmetry energy.
        - More protons: unstable, Coulomb force
        - More neutrons: unstable, symmetry energy

Any stable nucleus with pure neutron clusters? NO

BUT we can find it in our Universe, NEUTRON STAR

Nuclear symmetry energy in neutron star

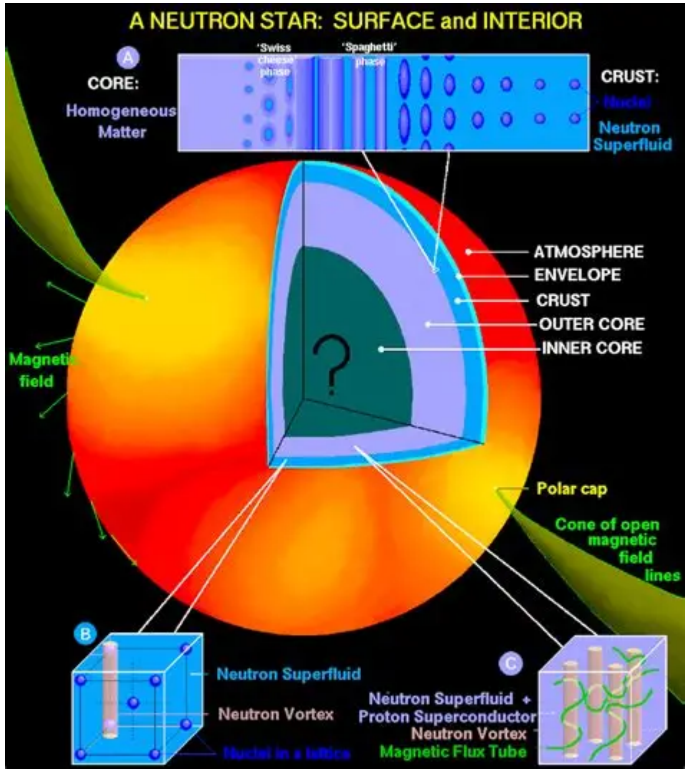

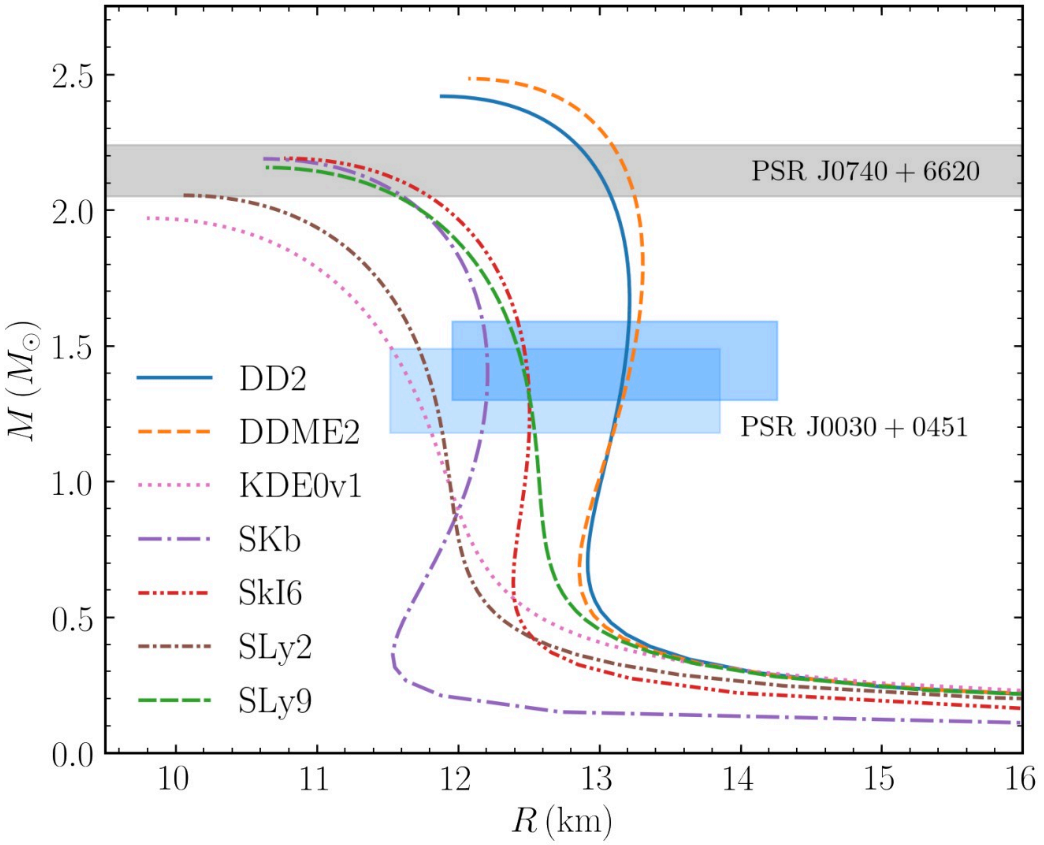

- Stiff symmetry energy: large L , more pressure from E_{sym} against gravity, large size
- Soft symmetry energy: small L , no enough pressure from E_{sym} against gravity, small size

E_{sym} measurement with neutron star (GW170817)

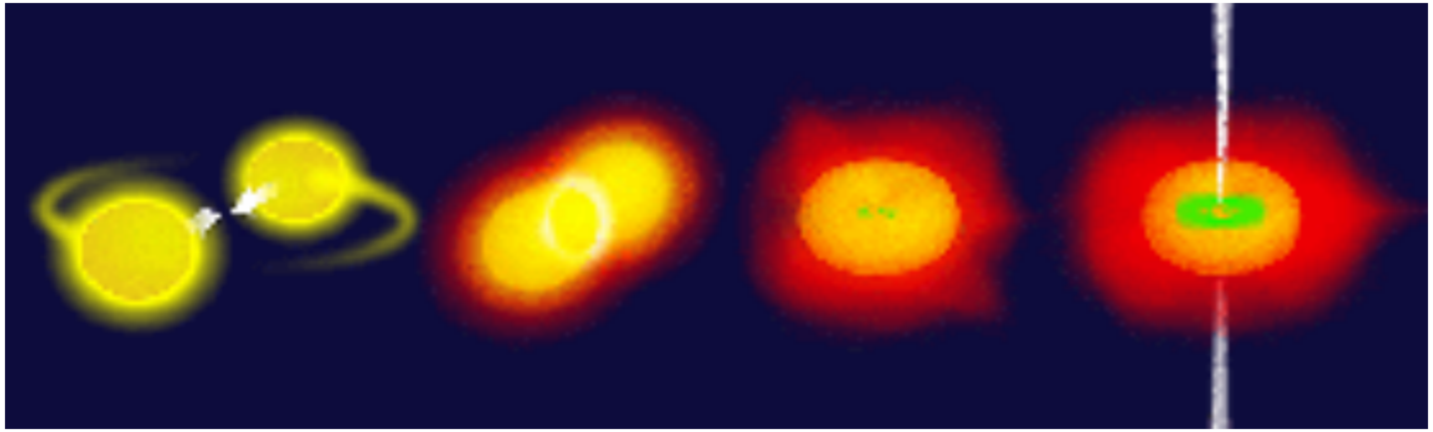

Neutron star merge

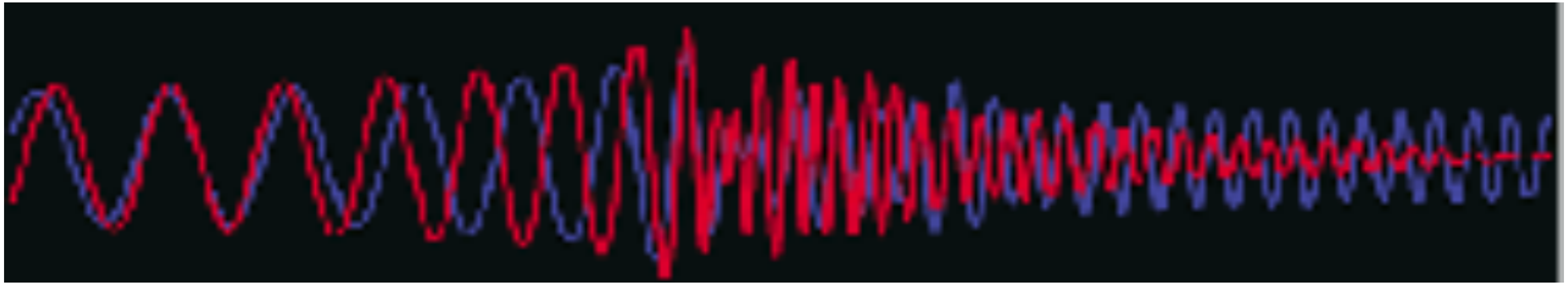

Tidal deformation

Selected for a Viewpoint in *Physics*

PRL **119,** 161101 (2017) PHYSICAL REVIEW LETTERS week ending 20 OCTOBER 2017

GW170817: Observation of Gravitational Waves from a Binary Neutron Star Inspiral

B. P. Abbott *et al.**

(LIGO Scientific Collaboration and Virgo Collaboration)

9853 citations

E_{sym} measurement with heavy ion collisions

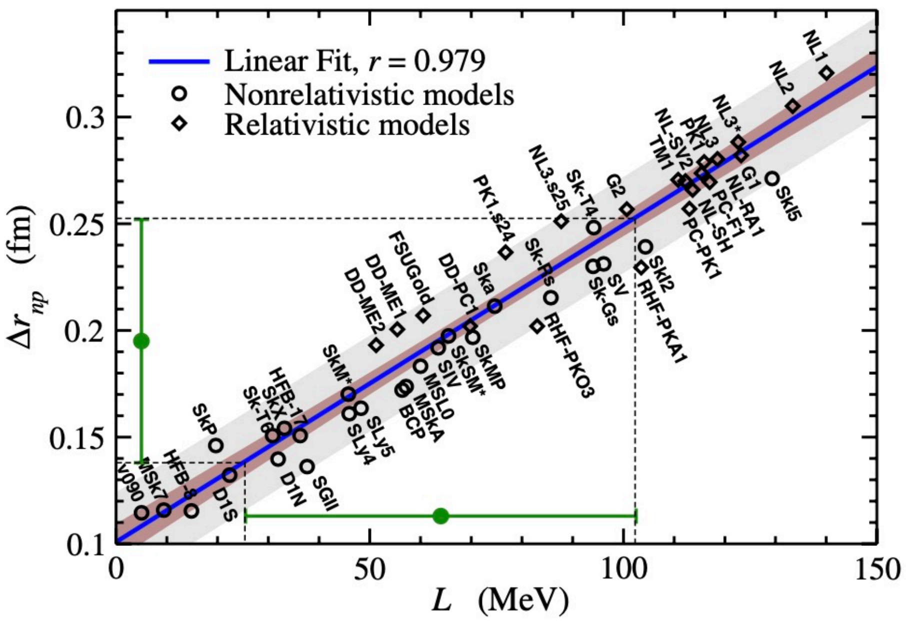

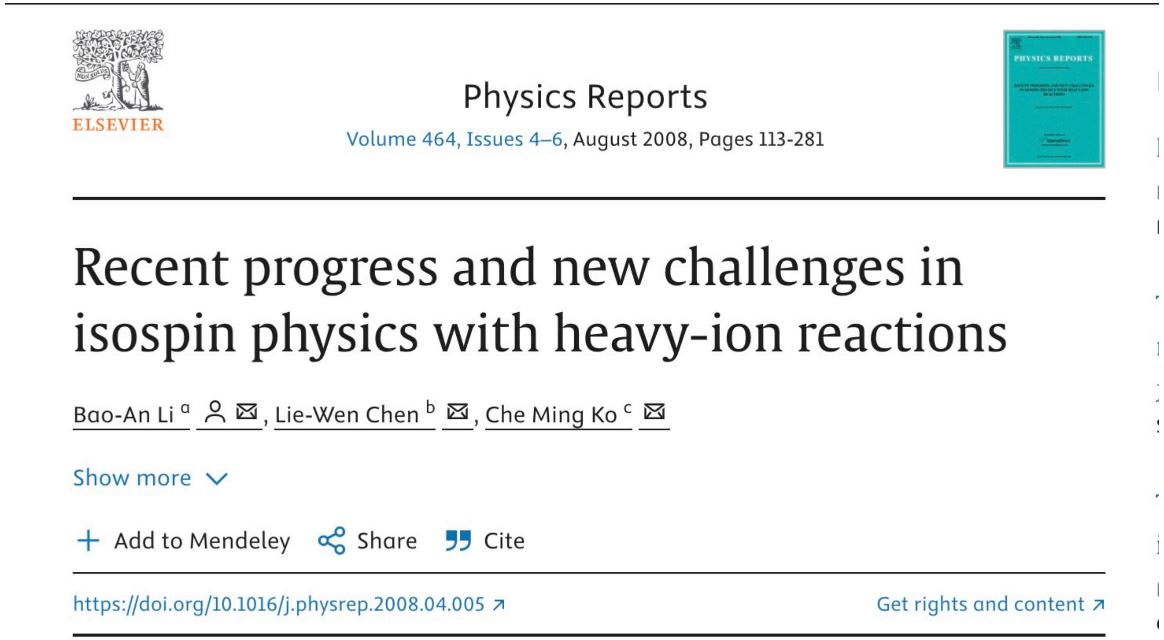
Physics Reports

Volume 464, Issues 4–6, August 2008, Pages 113-281

Recent progress and new challenges in isospin physics with heavy-ion reactions

Bao-An Li [a], Lie-Wen Chen [b], Che Ming Ko [c]

Show more

Add to Mendeley Share Cite

https://doi.org/10.1016/j.physrep.2008.04.005

Get rights and content

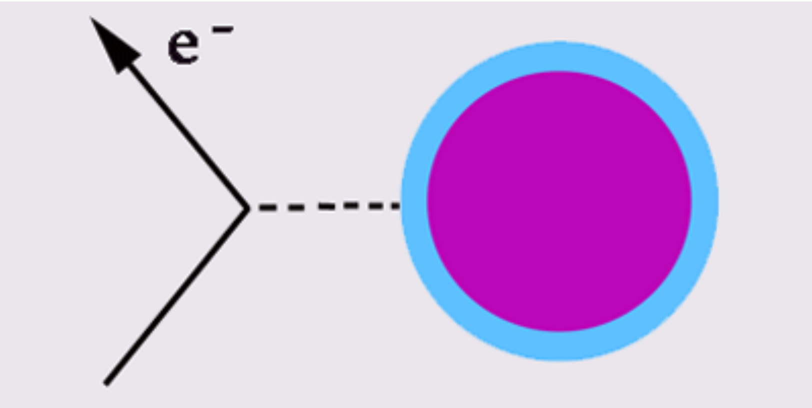

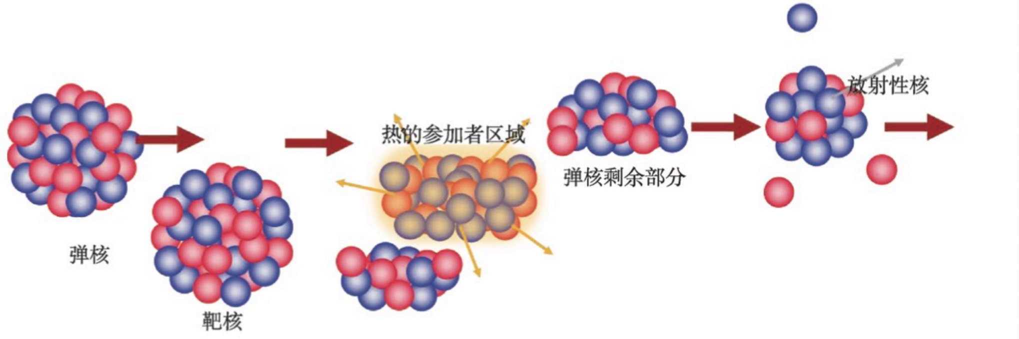

Nuclear symmetry energy on the earth

B. Li, et.al, Universe 7, 182 (2021)

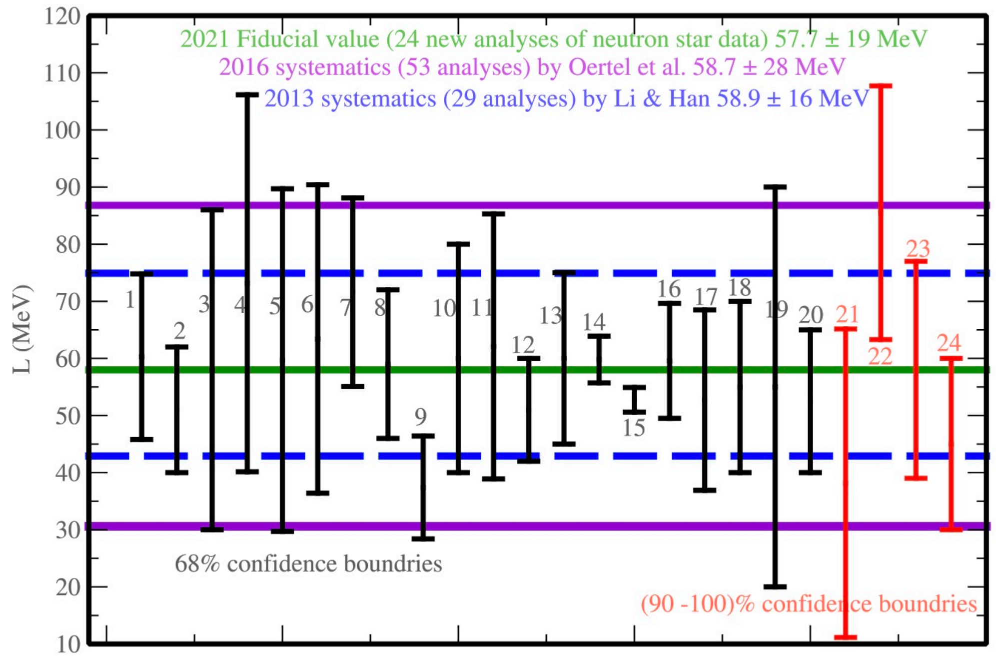

CREX Collaboration, PRL129, 042501 (2022)

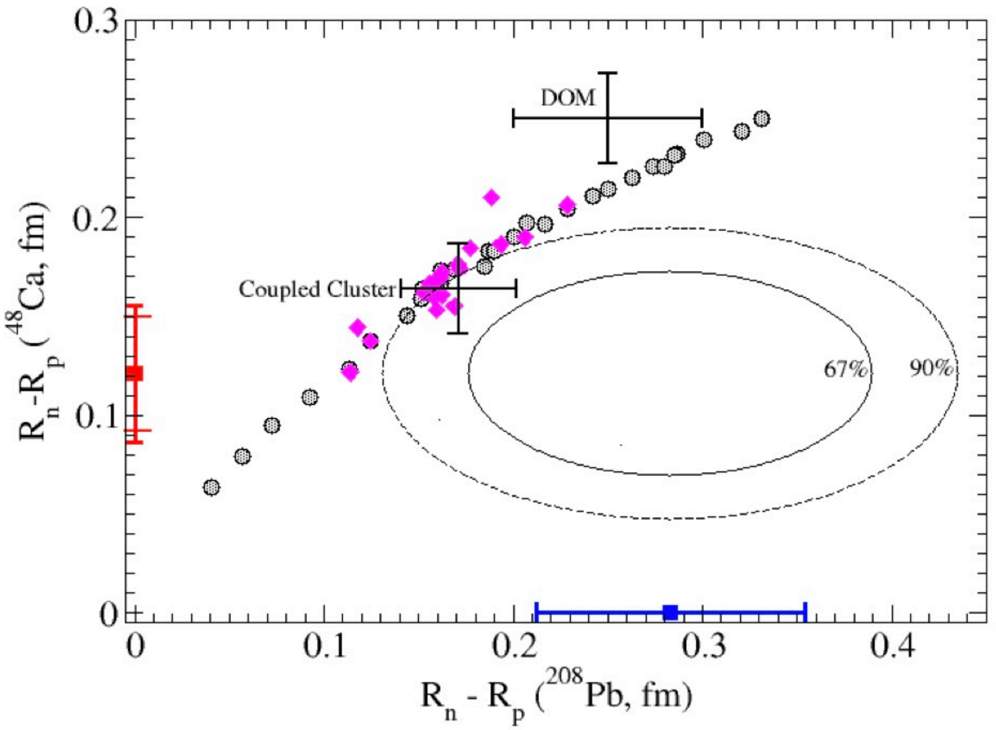

Symmetry energy is transitionally measured by low energy nuclear experiment. Over many decades, the issue is still not fully settled; e.g. world average L parameter is about 50 MeV, PREX electroweak measurement favors 100 MeV whereas CREX favors 30 MeV.

HIC vs relativistic HIC

G. Jin, Modern Physics

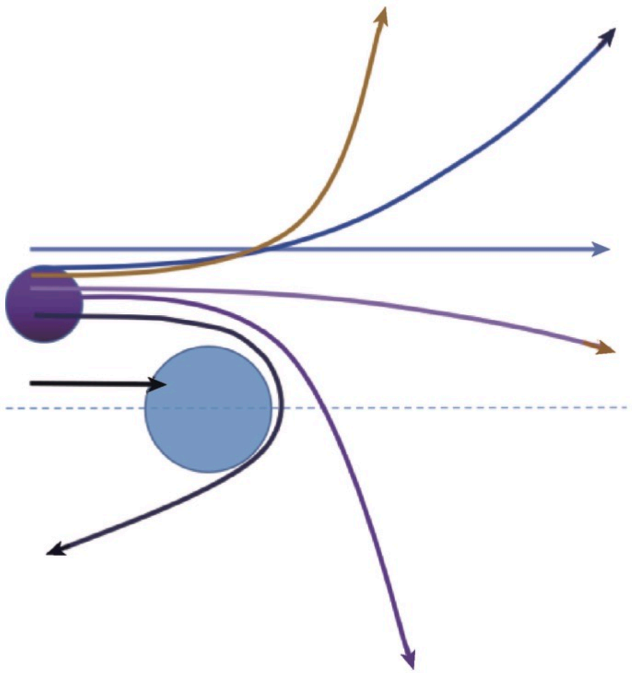

Hard scattering

$\sqrt{s} < \text{GeV}$

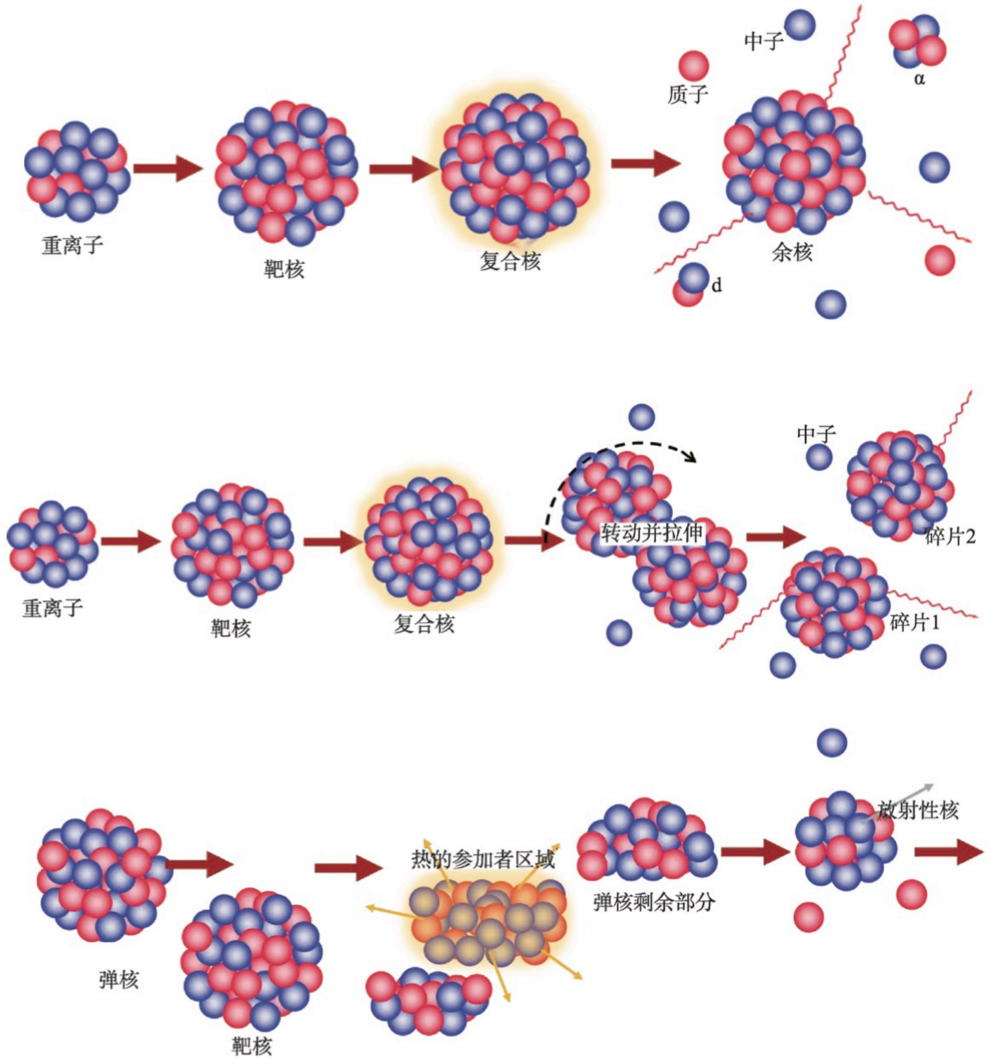

nuclear evaporation

fragmentation

projectile fragmentation

Relativistic heavy ion collisions

The "Little Bang"

$\sqrt{s} = 100\text{GeV} \sim \text{TeV}$

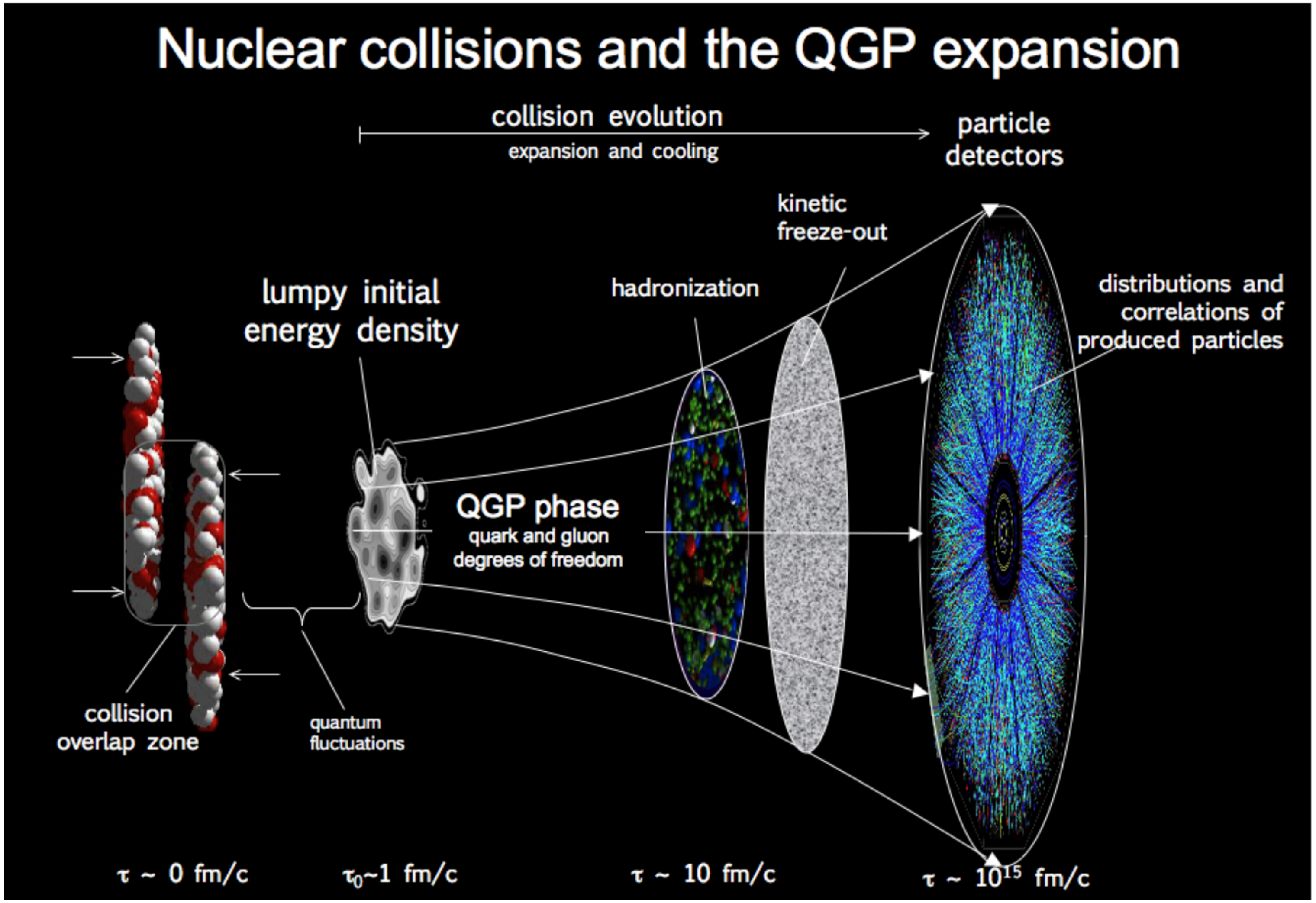

Yoctosecond (10^{-24} s) 幺秒

Relativistic heavy ion collisions

Participants

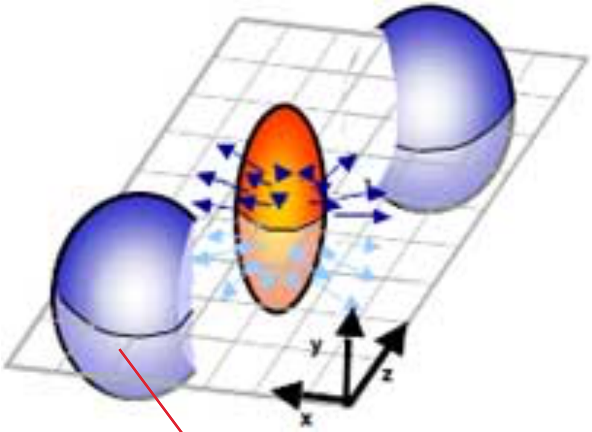

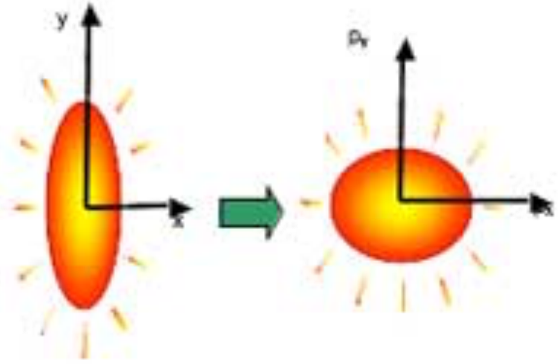

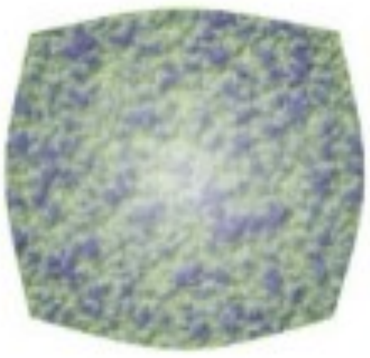

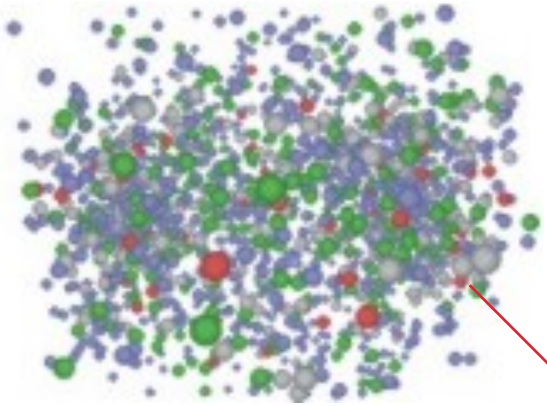

Chiral Magnetic Effect

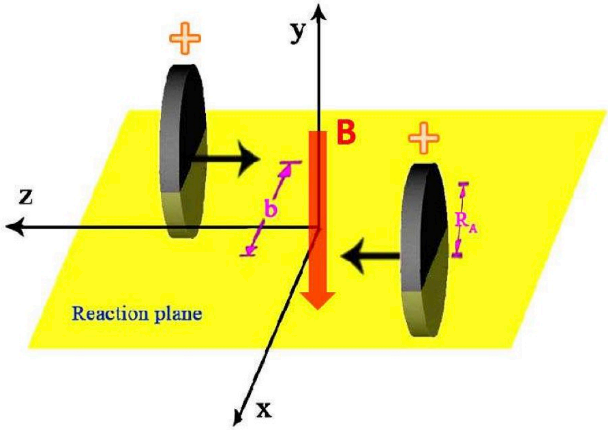

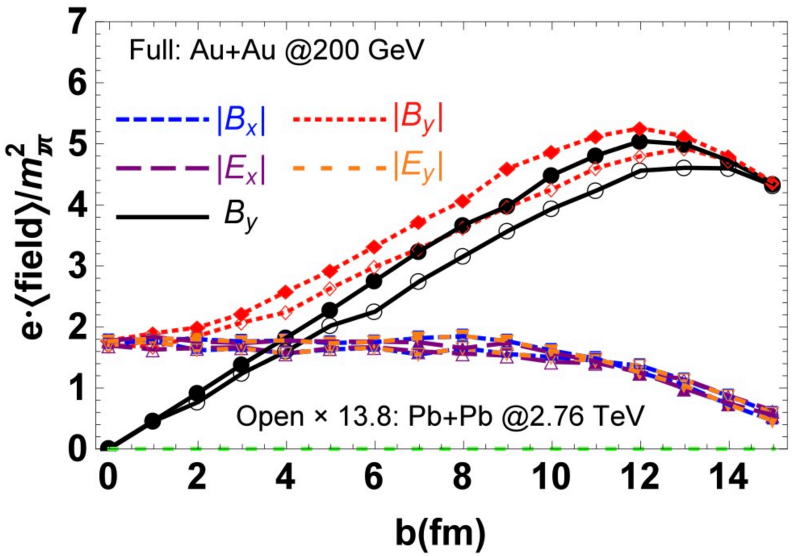

Spectators

Relativistic isobaric collisions and chiral magnetic effect

Chiral magnetic effect (CME)

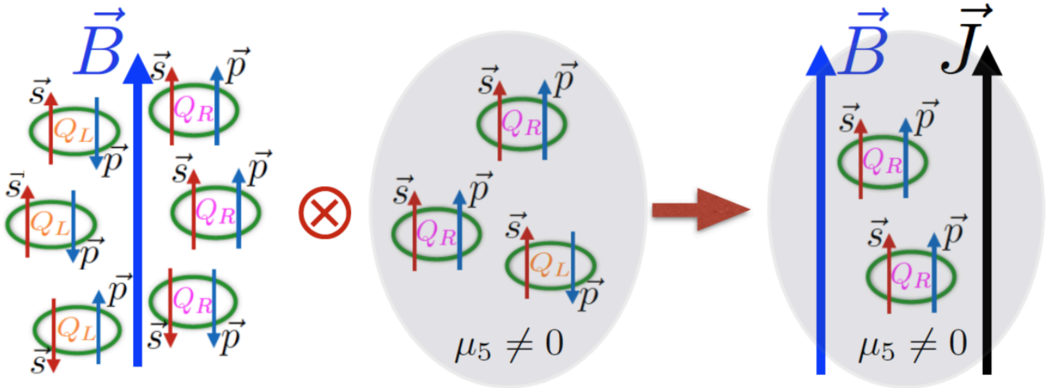

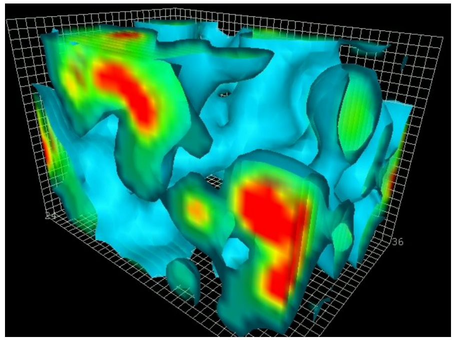

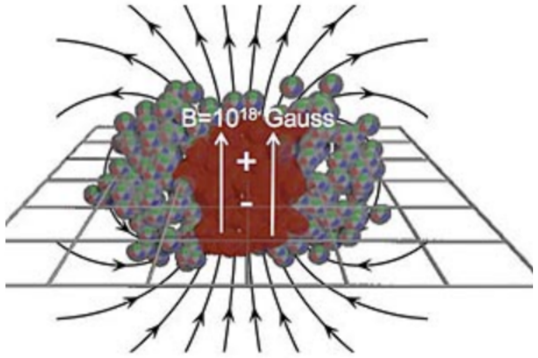

$$\mathbf{J_{cme}} = \sigma_5 \mathbf{B} = \left(\frac{(Qe)^2}{2\pi^2} \mu_5 \right) \mathbf{B},$$

D. Kharzeev,et.al., PPNP88, 1(2016)

The isobar collisions was proposed to measure the chiral magnetic effect.

S. Voloshin, PRL105, 172301 (2010)

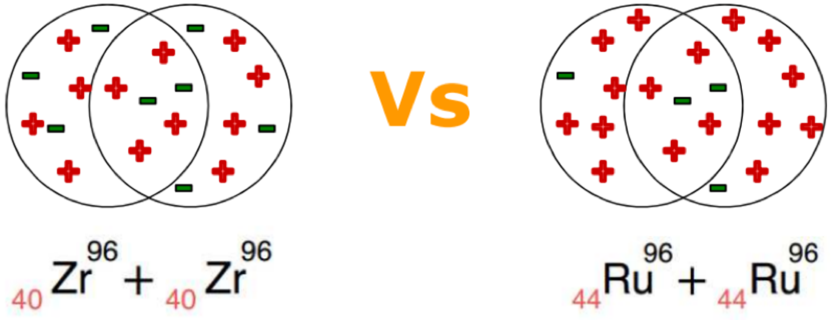

- Same background
- Different magnetic field => different CME signals

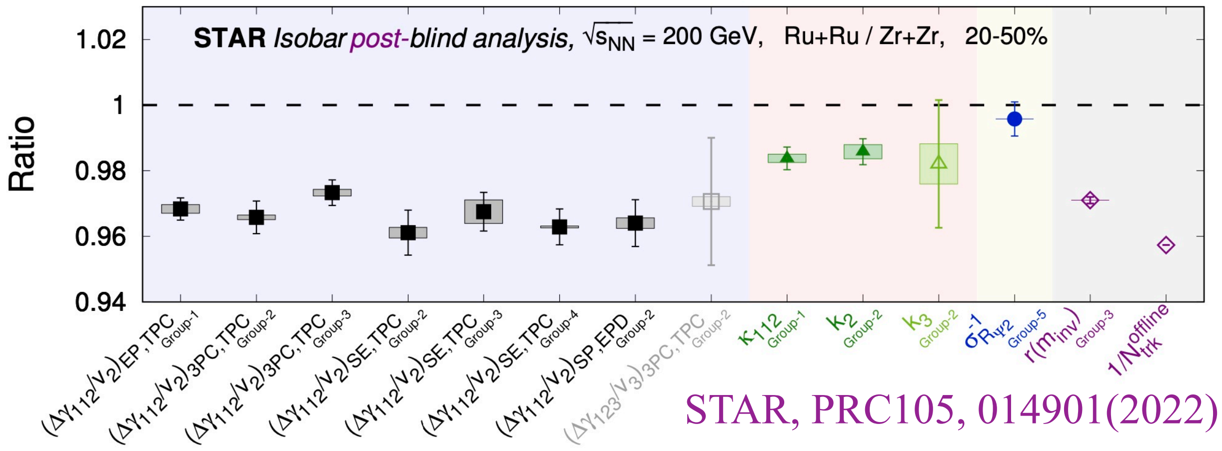

STAR, PRC105, 014901(2022)

Backgrounds are not identical!!!

Isobar structures are important for the CME search

STAR Collaboration, PRC105, 014901 (2022)

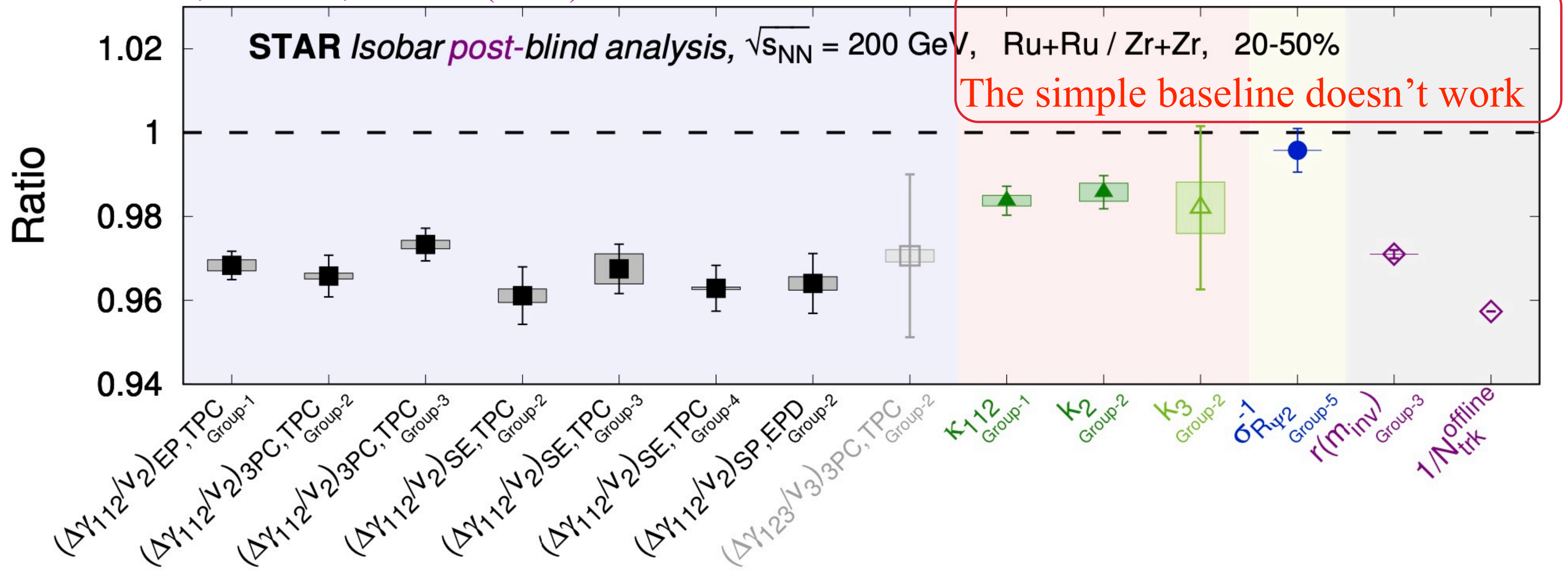

$$\Delta\gamma_{\rm bkg} = \langle \cos(\varphi_\alpha + \varphi_\beta - 2\Psi_{RP}) \rangle = \frac{N_{\rm cluster}}{N_\alpha N_\beta} \times \langle \cos(\varphi_\alpha + \varphi_\beta - 2\Psi_{\rm cluster}) \times v_{2,\rm cluster} \rangle$$

Multiplicity differences

Flow differences

The multiplicity and v2 differences from isobar structure are crucial for the CME search in the isobar collisions at RHIC

Nuclear densities for HIC models

PHYSICAL REVIEW LETTERS **121,** 022301 (2018)

Instead of WS densities, we use the nuclear densities obtained from density functional theory calculations

Importance of Isobar Density Distributions on the Chiral Magnetic Effect Search

Hao-jie Xu,[1] Xiaobao Wang,[1] Hanlin Li,[2] Jie Zhao,[3] Zi-Wei Lin,[4,5] Caiwan Shen,[1] and Fuqiang Wang[1,3,*]

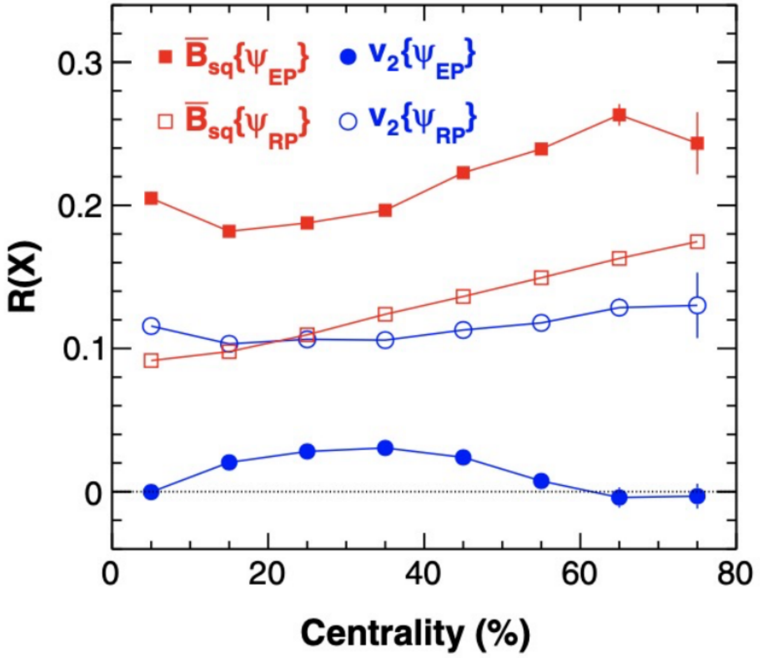

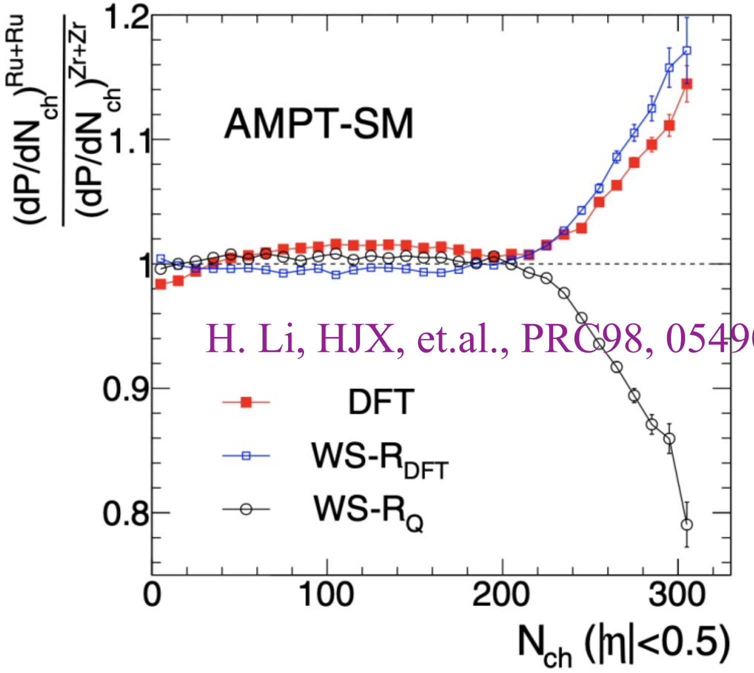

H. Li, HJX, et.al., PRC98, 054907 (2018)

DFT predictions are verified by STAR data

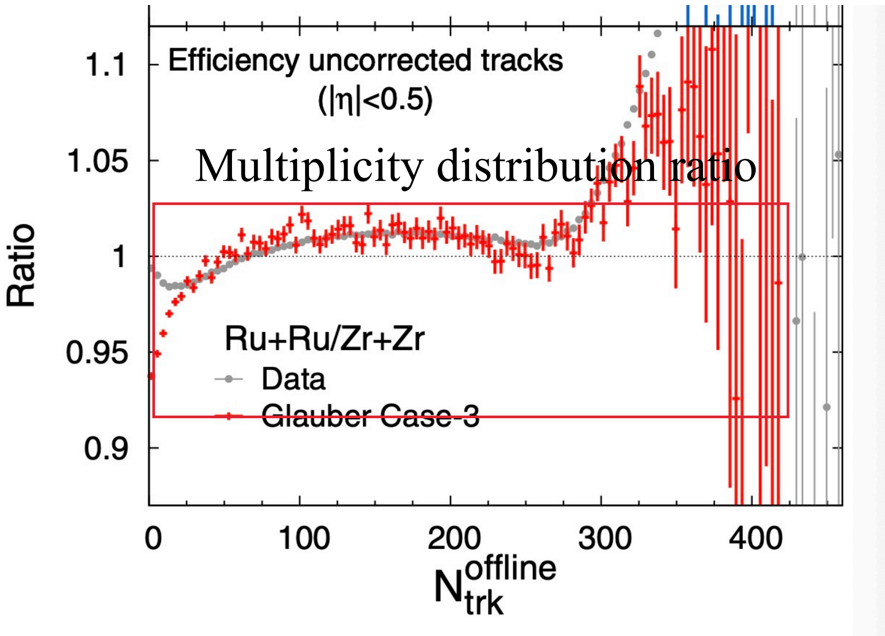

STAR, PRC105, 014901(2022)

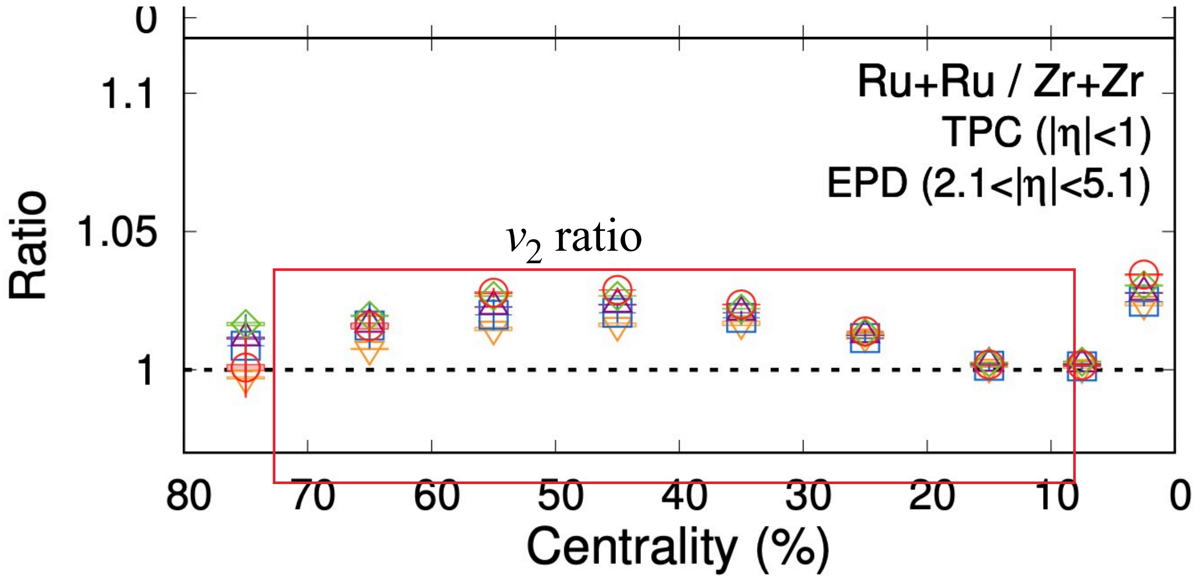

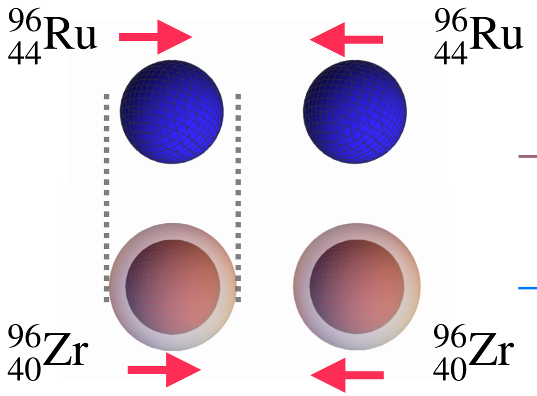

Neutron skin thickness $\Delta r_{np} \equiv \sqrt{\langle r_n^2 \rangle} - \sqrt{\langle r_p^2 \rangle}$

→ Smaller r, larger density → Larger N_{ch} and $\langle p_T \rangle$

→ Larger r, smaller density → Smaller N_{ch} and $\langle p_T \rangle$

Determine the neutron skin type by STAR data

HJX, et.al., PLB819, 136453 (2021)

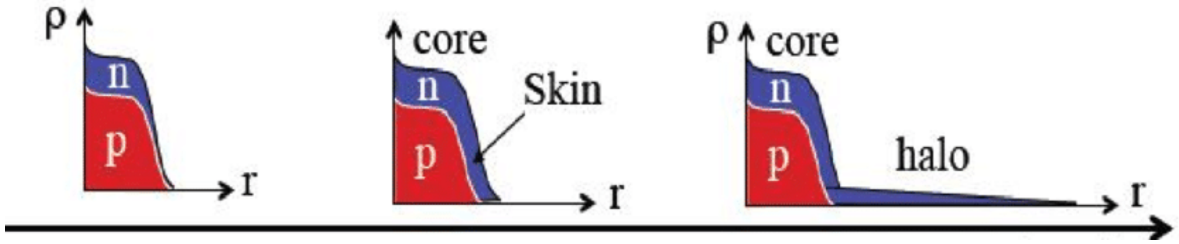

- Neutron-skin nuclei and neutron-halo nuclei for Zr

	^{96}Ru		^{96}Zr	
	R	*a*	*R*	*a*
p	5.085	0.523	5.021	0.523
skin-type n	5.085	0.523	5.194	0.523
halo-type n	5.085	0.523	5.021	0.592

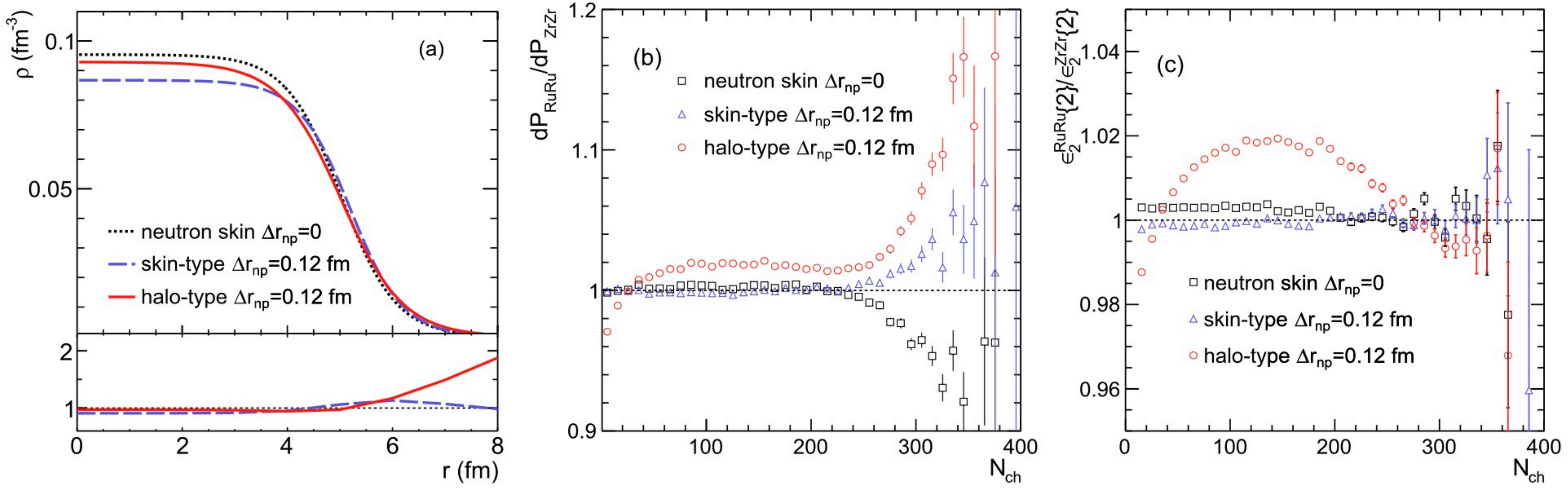

The shapes of the Ru+Ru/Zr+Zr ratios of the multiplicity and eccentricity in mid-central collisions can further distinguish between skin-type and halo-type neutron densities.

Neutron skin and nuclear symmetry energy

Z. Zhang, PRC94, 064326(2016)
H. Li, HJX, et.al., PRL125, 222301(2020)

SHF: Standard Skyrme-Hartree-Fock (SHF) model
eSHF: Extended SHF model

$$
\begin{aligned}
v_{i,j} &= t_0(1+x_0P_\sigma)\delta(\boldsymbol{r}) + \frac{1}{6}t_3(1+x_3P_\sigma)\rho^\alpha(\boldsymbol{R})\delta(\boldsymbol{r}) \\
&+ \frac{1}{2}t_1(1+x_1P_\sigma)[K'^2\delta(\boldsymbol{r}) + \delta(\boldsymbol{r})K^2] \\
&+ t_2(1+x_2P_\sigma)\boldsymbol{K}'\cdot\delta(\boldsymbol{r})\boldsymbol{K} \\
&+ \frac{1}{2}t_4(1+x_4P_\sigma)[K'^2\delta(\boldsymbol{r})\rho(\boldsymbol{R}) + \rho(\boldsymbol{R})\delta(\boldsymbol{r})K^2] \\
&+ t_5(1+x_5P_\sigma)\boldsymbol{K}'\cdot\rho(\boldsymbol{R})\delta(\boldsymbol{r})\boldsymbol{K} \\
&+ iW_0(\boldsymbol{\sigma}_i+\boldsymbol{\sigma}_j)\cdot[\boldsymbol{K}'\times\delta(\boldsymbol{r})\boldsymbol{K}], \qquad (4)
\end{aligned}
$$

Extended

$$E(\rho,\delta) = E_0(\rho) + E_{\rm sym}(\rho)\delta^2 + O(\delta^4)$$

$$\rho = \rho_n + \rho_p;\ \ \delta = \frac{\rho_n - \rho_p}{\rho}$$

$$L(\rho_c) = 3\rho_c\left[\frac{dE_{\rm sym}(\rho)}{d\rho}\right]_{\rho=\rho_c};\ \ \rho_c \simeq 0.11{\rm fm}^{-3}$$

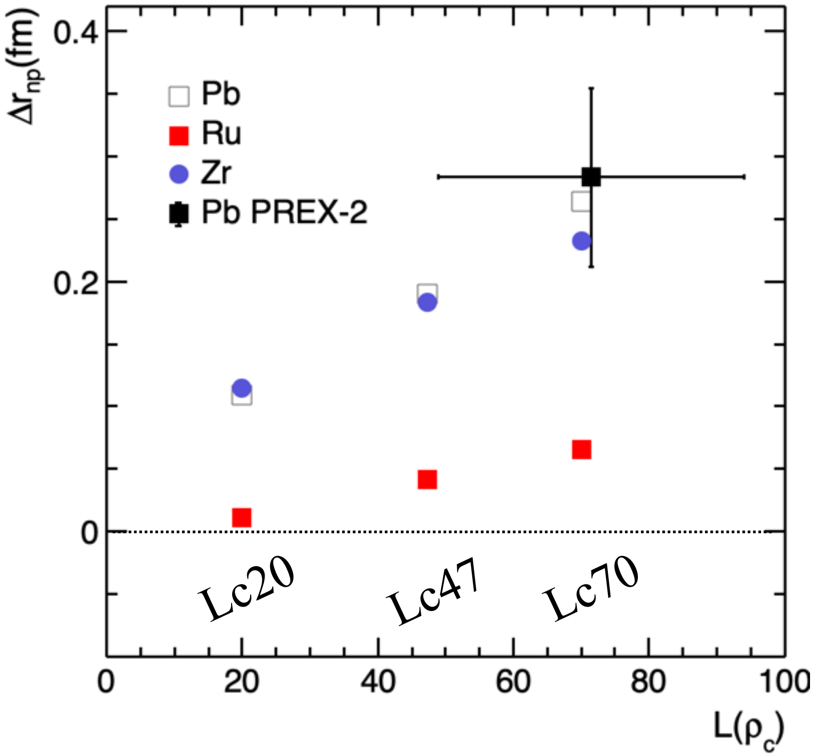

	$L(\rho_c)$	$L(\rho_0)$	^{96}Zr r_n	^{96}Zr r_p	^{96}Zr $\Delta r_{\rm np}$	^{96}Ru r_n	^{96}Ru r_p	^{96}Ru $\Delta r_{\rm np}$	^{208}Pb $\Delta r_{\rm np}$
Lc20	20	13.1	4.386	4.27	0.115	4.327	4.316	0.011	0.109
Lc47	47.3	55.7	4.449	4.267	0.183	4.360	4.319	0.042	0.190
Lc70	70	90.0	4.494	4.262	0.232	4.385	4.32	0.066	0.264
SLy4	42.7	46.0	4.432	4.271	0.161	4.356	4.327	0.030	0.160

Method I: multiplicity distribution ratio

H. Li, HJX, et.al., PRL125, 222301(2020)

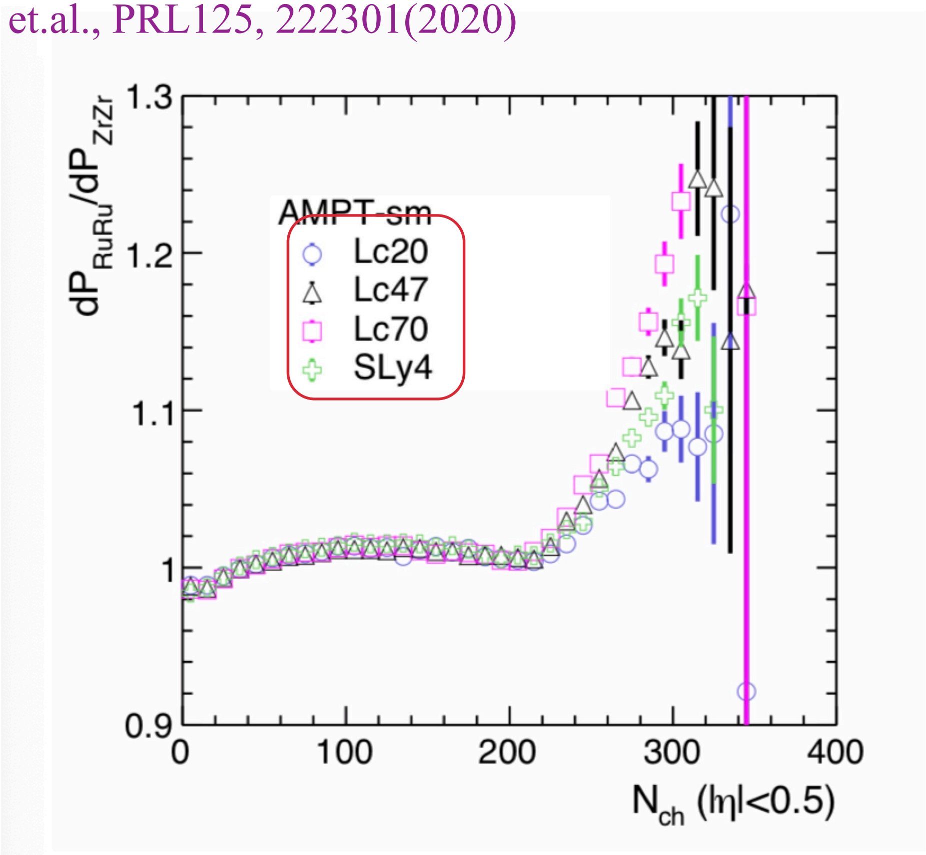

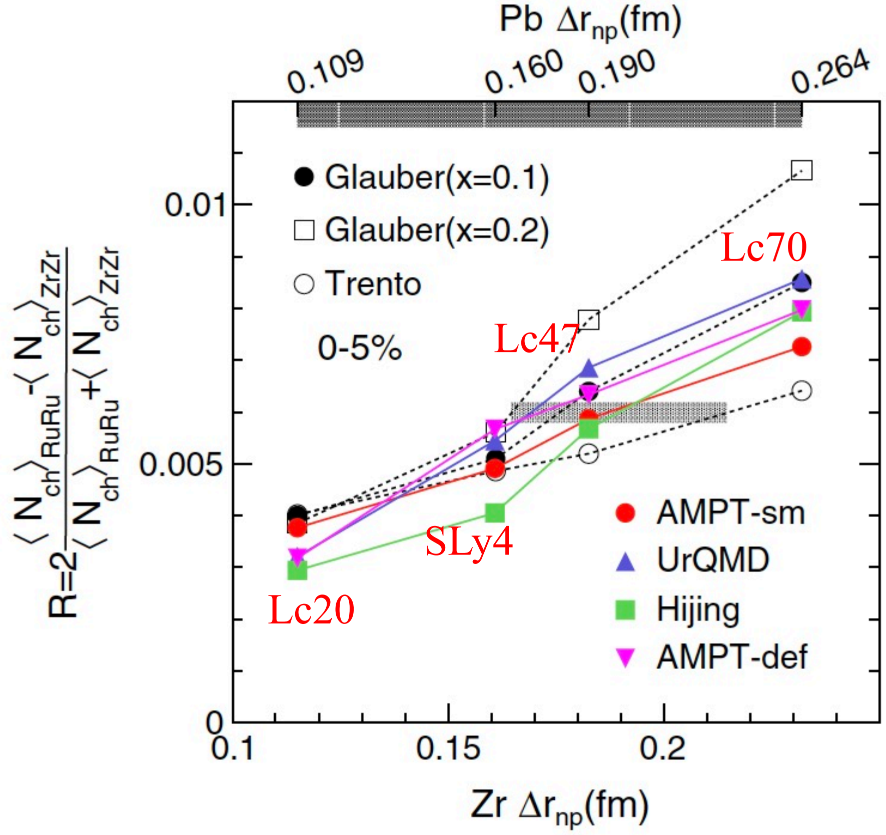

- The ratio of N_{ch} distributions highlight the differences
- To quantify the differences, we use the R observable of N_{ch} at top 5% centrality.
- R is a relative measure, **much of experimental effects cancel**

Method II: mean p_T ratio

HJX, et.al., PRC108, L011902 (2023)

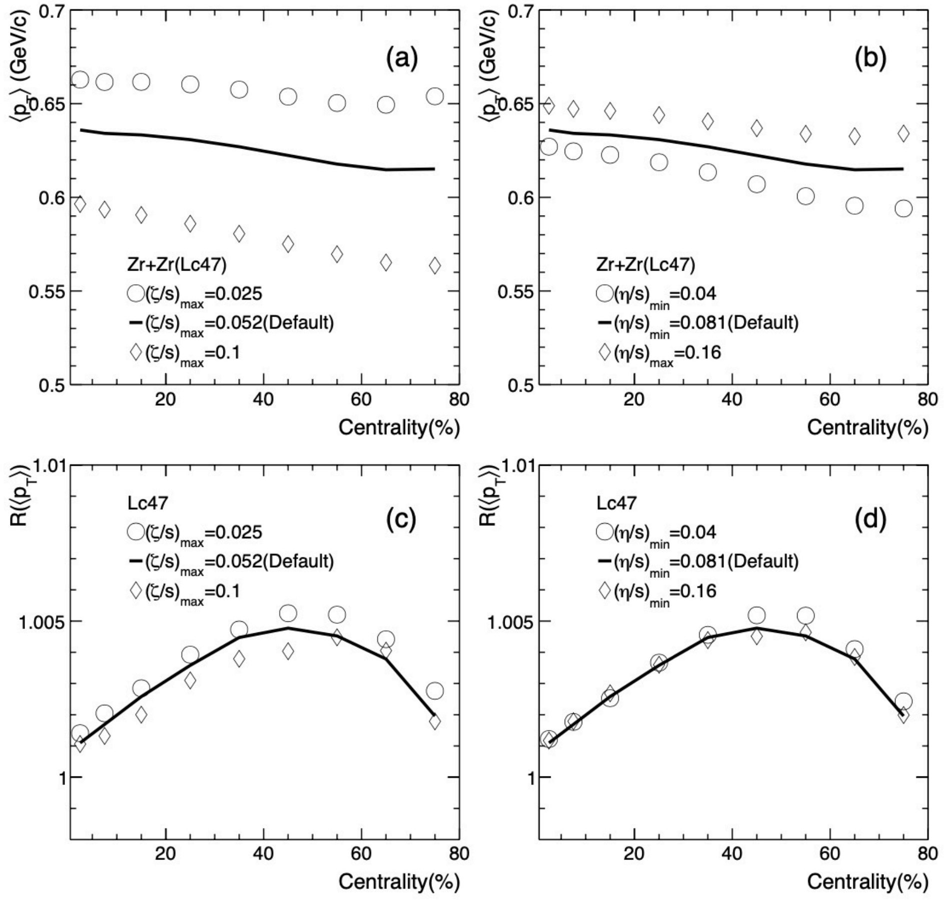

$$R(\langle p_T \rangle) \propto R(d_\perp) \propto 1/R(\langle \sqrt{r^2} \rangle)$$

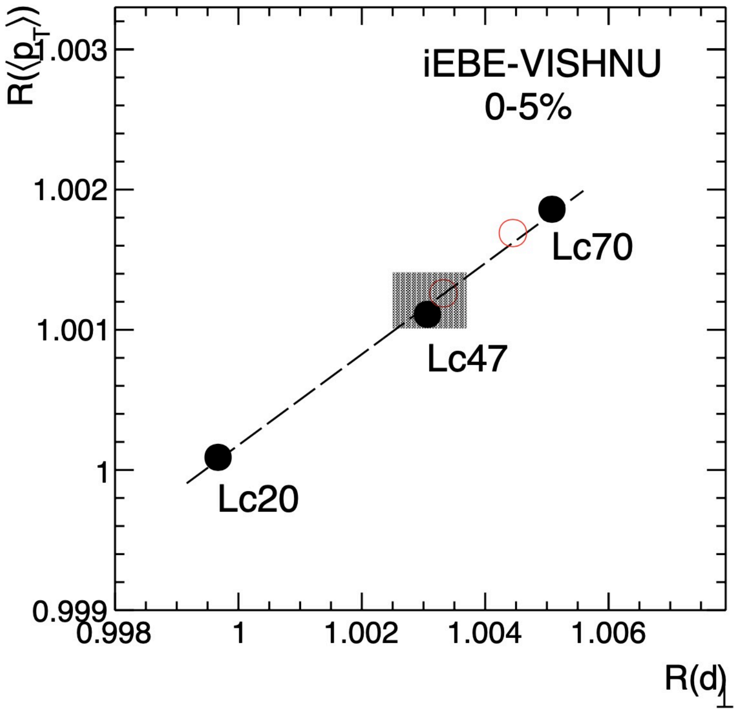

The $R(\langle p_T \rangle)$ is inversely proportional to nuclear size ratio in most central collisions.

Method III: net-charge ratio in very peripheral collisions

HJX, et.al., PRC105, L011901 (2022)

For the colliding nuclei with large neutron skin thickness

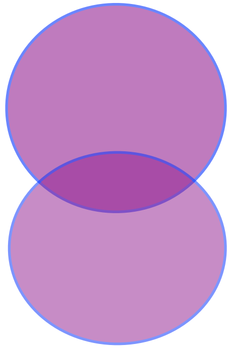

→ more n+n collisions at most peripheral collisions → Less participant charges, thus less final net-charges

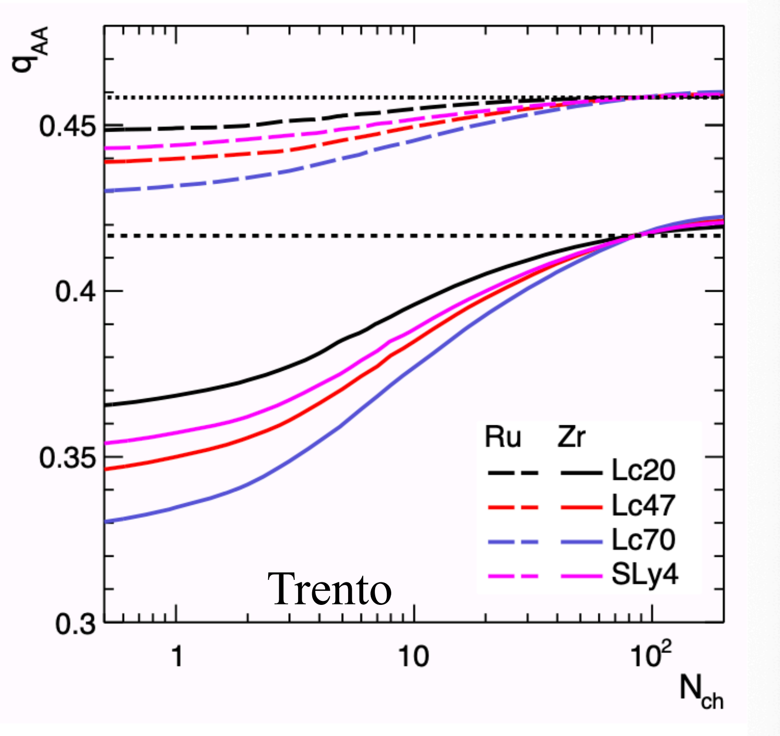

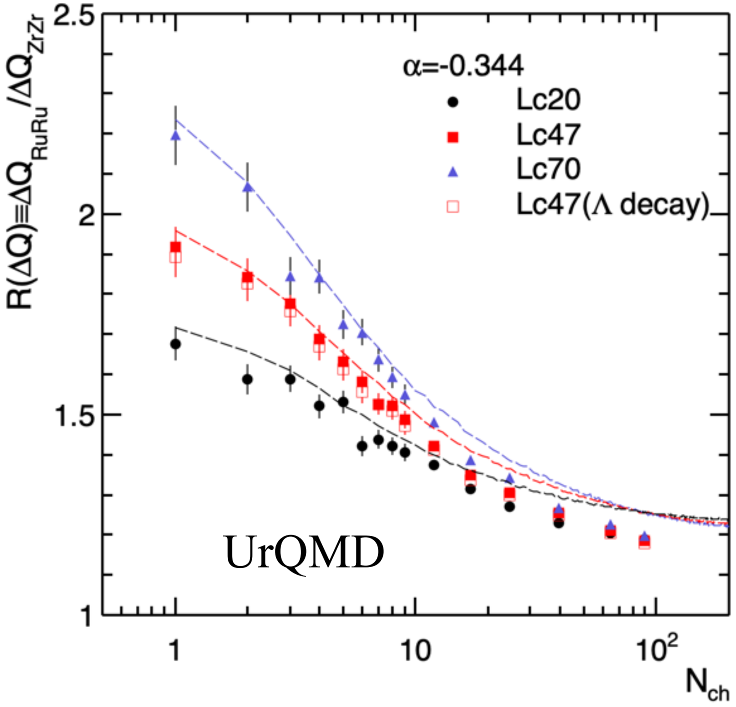

The curves are calculated by superimposition assumption

$$R(\Delta Q) = \frac{q_{\mathrm{RuRu}} + \alpha/(1-\alpha)}{q_{\mathrm{ZrZr}} + \alpha/(1-\alpha)}$$

where $q_{\mathrm{RuRu/ZrZr}}$ are the fraction of protons among the participant nucleons, obtained by the Trento model.

α is the ΔQ ratio in nn to pp interaction:

Pytha: $\alpha = -0.352$

Hijing: $\alpha = -0.389$

UrQMD: $\alpha = -0.344$

Method IV: spectator neutrons in ultracentral collisions

L. Liu, et.al, PLB, 834, 137441(2022)

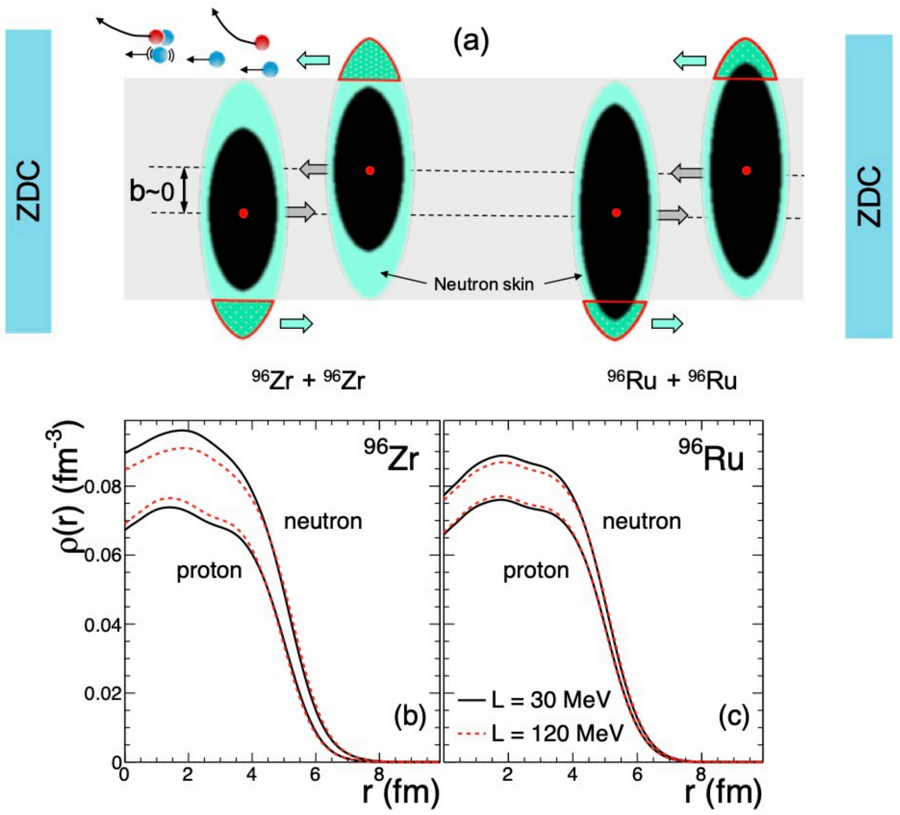

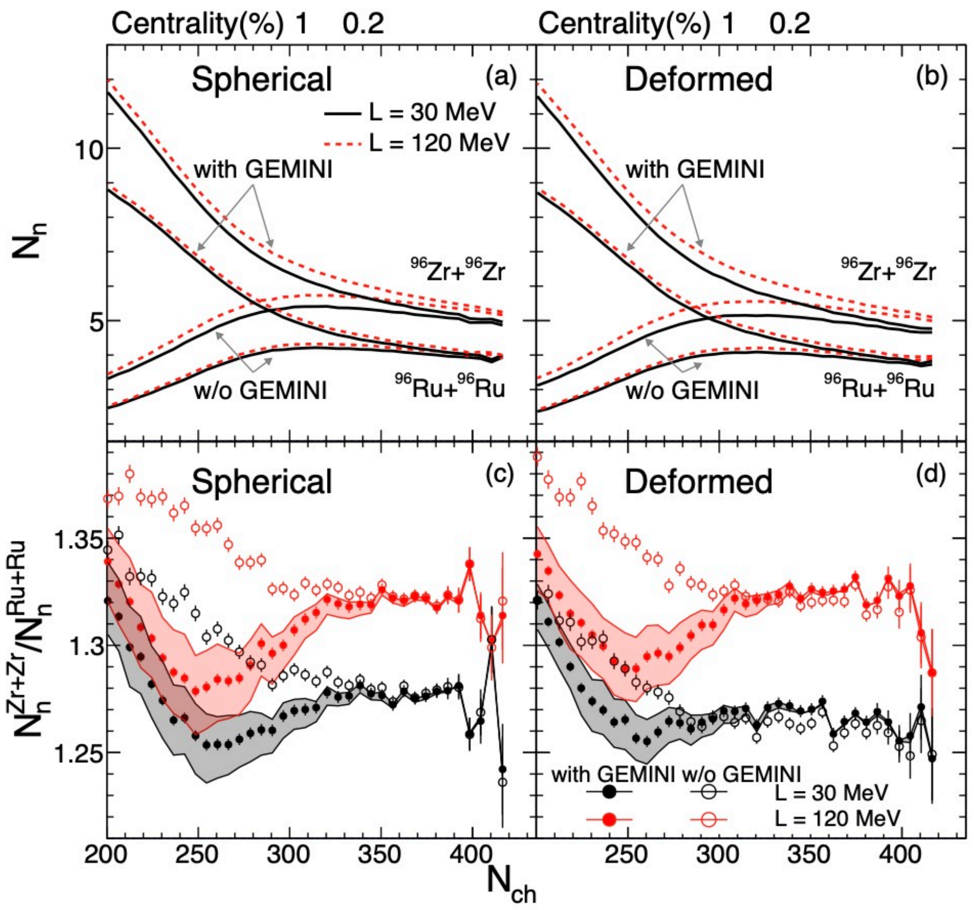

The yield ratio of free spectator neutrons is a clean probe of the neutron-skin thickness

STAR measurements

Compare to world wide data

State-of-the-art **spherical** DFT with eSHF nuclear potential

Zhang, Chen, PRC94, 064326 (2016)

- Multiplicity ratio:

  $L(\rho_c) = 53.8 \pm 1.7 \pm 7.8$ MeV

  $L(\rho) = 65.4 \pm 2.1 \pm 12.1$ MeV

  $\Delta r_{\mathrm{np,Zr}} = 0.195 \pm 0.019$ fm

  $\Delta r_{\mathrm{np,Ru}} = 0.051 \pm 0.009$ fm

- $\langle p_T \rangle$ ratio:

  $L(\rho_c) = 56.8 \pm 0.4 \pm 10.4$ MeV

  $L(\rho) = 69.8 \pm 0.7 \pm 16.0$ MeV

  $\Delta r_{\mathrm{np,Zr}} = 0.202 \pm 0.024$ fm

  $\Delta r_{\mathrm{np,Ru}} = 0.052 \pm 0.012$ fm

B. Li, et.al Universe 7, 182 (2021)

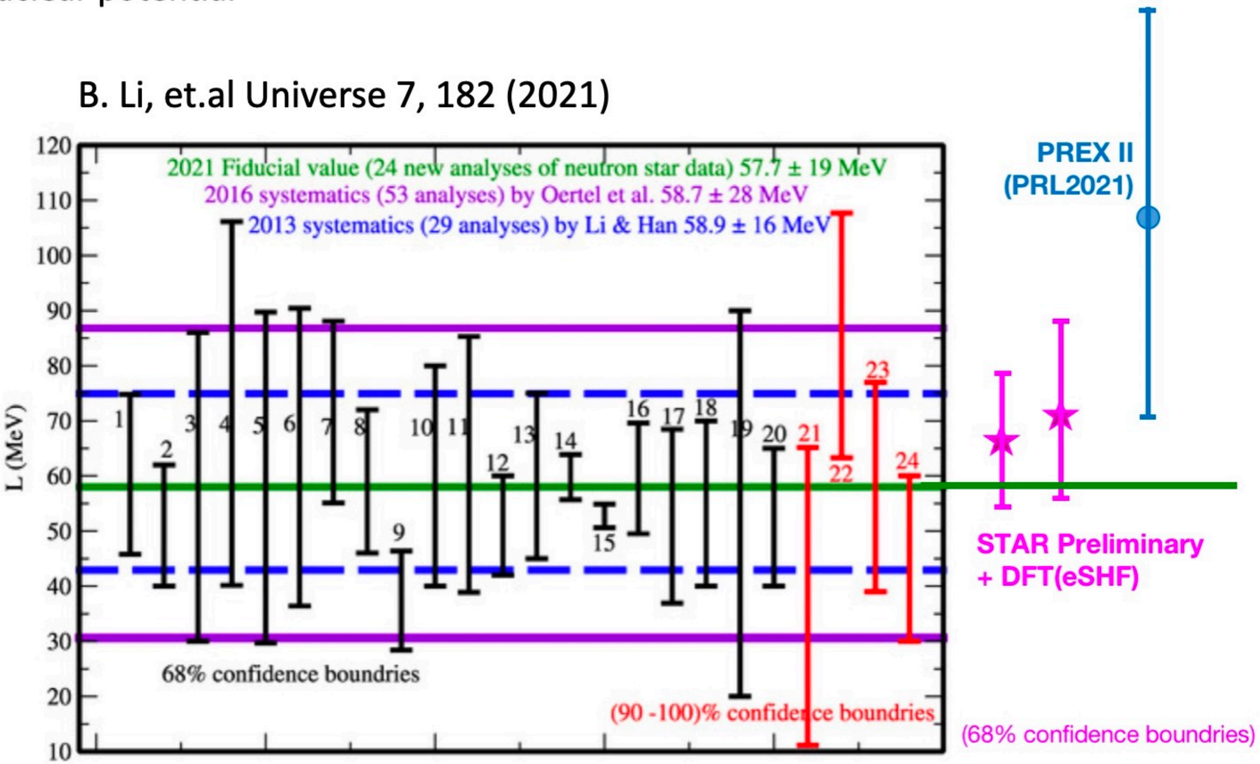

Consistent with world wide data with good precision

Relativistic hydrodynamic model

Supplementary Table 1 | Summary of estimated parameters

Parameter	Description	Prior range	Posterior estimate	MAP value
Norm [GeV]	Normalization factor, $\sqrt{s_{NN}}$ = 2.76 TeV	8–20	$13.9^{+1.2}_{-1.1}$	13.94
Norm [GeV]	Normalization factor, $\sqrt{s_{NN}}$ = 5.02 TeV	10–25	$18.5^{+1.8}_{-1.7}$	18.38
p	Energy deposition parameter	−1/2 to +1/2	$0.006^{+0.078}_{-0.078}$	0.007
σ_{fluct}	Std. dev. of nucleon multiplicity fluctuations	0–2	$0.90^{+0.24}_{-0.27}$	0.918
w [fm]	Gaussian nucleon width	0.4–1.0	$0.96^{+0.04}_{-0.05}$	0.956
d_{min} [fm]	Minimum inter-nucleon distance	0–1.7	$1.28^{+0.42}_{-0.53}$	1.27
τ_{fs} [fm/c]	Free streaming time	0–1.5	$1.16^{+0.29}_{-0.25}$	1.16
η/s min	Minimum value of η/s (at T_c)	0–0.2	$0.085^{+0.026}_{-0.025}$	0.081
η/s slope [GeV^{-1}]	Slope of η/s above T_c	0–8	$0.83^{+0.83}_{-0.83}$	1.11
η/s crv	Curvature of η/s above T_c	−1 to +1	$-0.37^{+0.79}_{-0.63}$	−0.48
ζ/s max	Maximum value of ζ/s	0–0.1	$0.037^{+0.040}_{-0.022}$	0.052
ζ/s width [GeV]	Width of ζ/s peak	0–0.1	$0.029^{+0.045}_{-0.026}$	0.022
ζ/s T_{peak} [GeV]	Temperature of ζ/s maximum	0.150–0.200	$0.177^{+0.023}_{-0.021}$	0.183
T_{switch} [GeV]	Switching / particlization temperature	0.135–0.165	$0.152^{+0.003}_{-0.003}$	0.151

Posterior estimates: The central values are the medians; uncertainties are the 90% highest posterior density (HPD) credible intervals. The maximum a posteriori (MAP) values were determined by numerically maximizing the posterior probability.

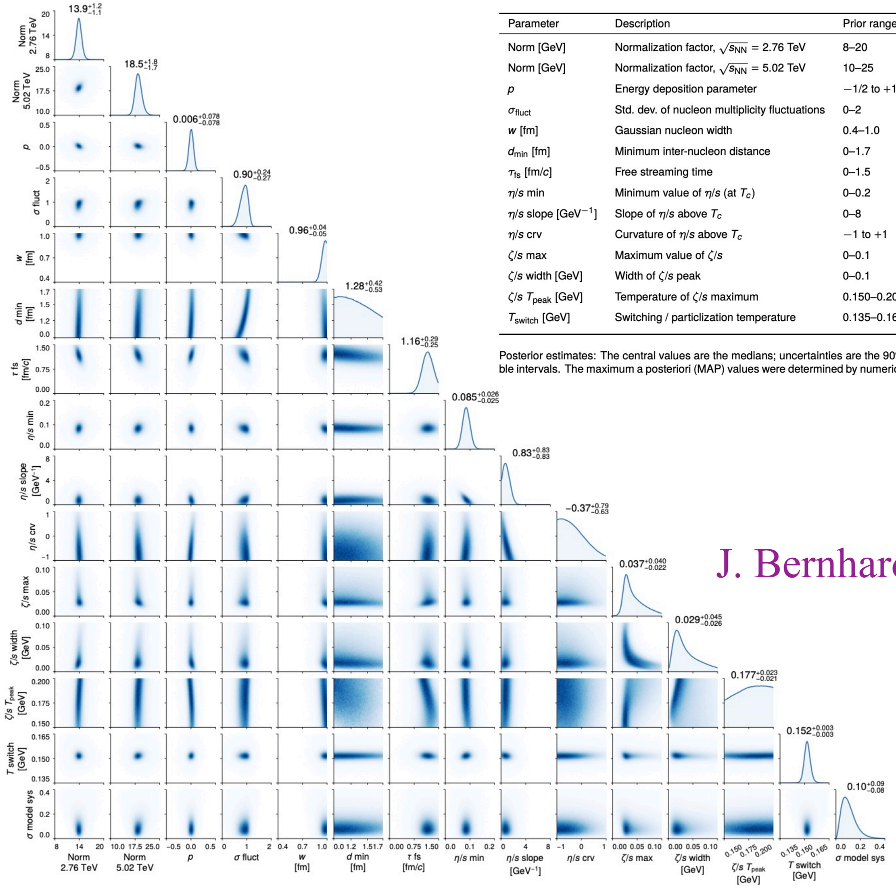

Supplementary Fig. 2 | Posterior distribution for all parameters. Diagonal: Marginal distributions (histograms) for each parameter. Annotated are the posterior medians and 90% highest posterior density (HPD) credible intervals. Off-diagonal: Joint distributions (density histograms) showing correlations between pairs of parameters.

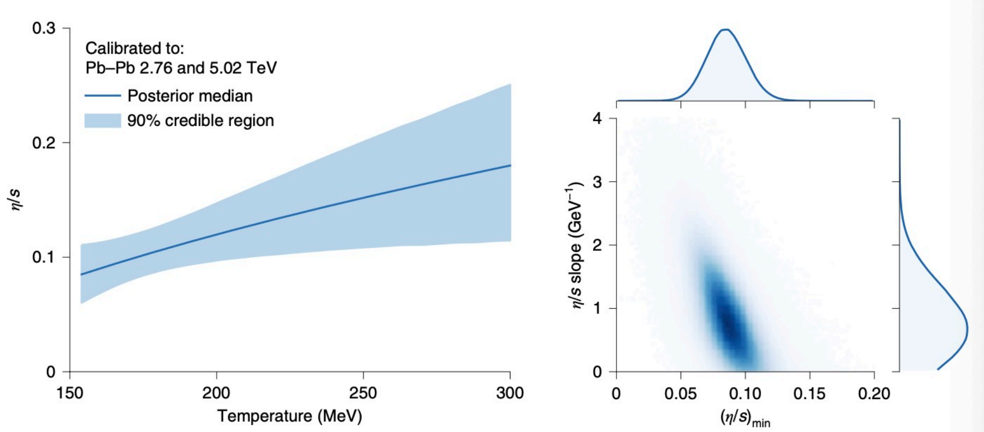

J. Bernhard, et.al, Nature Physics, 15 ,1113-1117

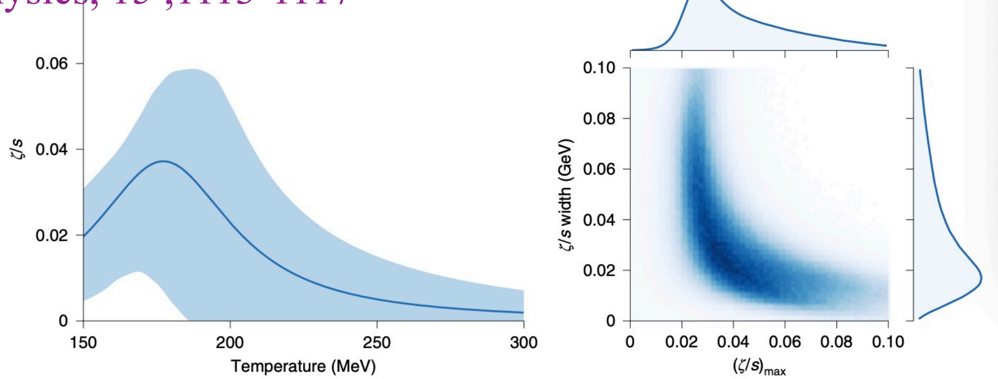

Proceed with extreme caution when extracting anything from the single collision system!

SUMMARY

- The nuclear symmetry energy is important for both finite nuclei and neutron star
- CME background in relativistic isobar collisions depend on nuclear symmetry energy
- Unconventional way to **probe the neutron skin and symmetry energy**

Thank you for your attention!

Haojie Xu(徐浩洁)

Huzhou University(湖州师范学院)